

轴肩下压量对搅拌摩擦焊搭接接头力学性能的影响

邢 丽, 魏 鹏, 宋 骁, 柯黎明

(南昌航空大学 轻合金加工科学与技术国防重点学科实验室, 南昌 330063)

摘 要: 采用表面为右螺纹圆柱型搅拌针的搅拌头对 3 mm 厚 LY12 铝合金进行了搅拌摩擦焊搭接试验, 研究了轴肩下压量对接头界面迁移和搭接接头力学性能的影响. 结果表明 随轴肩下压量增大, 焊缝两侧的搭接界面均向下迁移, 其迁移量随下压量的增加而增加, 焊缝返回侧的界面迁移量大于前进侧. 控制轴肩下压量, 当轴肩下压量合适时, 焊缝两侧的界面仅发生较小的迁移. 当焊缝两侧的界面仅发生较小的迁移量时, 搭接接头有较高的抗剪强度, 且断裂都发生在上板, 呈正断. 焊缝两侧的搭接界面向下迁移时, 断裂都发生在下板, 接头抗剪强度随界面迁移高度的增加而减小, 且受拉侧在下板前进侧时, 接头的抗剪强度较受拉侧在下板返回侧时的高.

关键词: 搅拌摩擦焊; 搭接接头; 轴肩下压量; 界面迁移; 力学性能

中图分类号: TG453 文献标识码: A 文章编号: 0253-360X(2013)03-0015-05



邢 丽

0 序 言

搅拌摩擦焊是英国焊接研究所(TWI)于1991年发明的一种新型的固相连接技术, 目前, 该技术在航天航空、船舶、汽车等领域已显示出广泛的应用前景^[1]. 在实际应用中, 搅拌摩擦焊除了能焊接对接接头, 还可焊接搭接或T形接头. 但在实践中, 搭接焊缝两侧的界面会发生向上或向下的迁移. 这种迁移的界面当接头承受载荷时, 不仅会减小接头的有效承载面积, 而且界面尖端处的缺口呈三向应力状态; 尤其当界面弯曲畸变程度比较严重、与接头受力方向垂直时, 会在接头处产生严重的应力集中^[2].

搅拌头形状和焊接工艺参数是影响界面迁移的两个重要因素. Xing和柯黎明等人^[3,4]研究了6种搅拌针形状对搭接界面迁移的影响, 发现搅拌针表面上的螺纹是影响搭接界面迁移的重要因素, 右螺纹所焊接头界面迁移高度小于左螺纹, 接头强度较高. Lee和魏鹏等人^[5,6]采用左螺纹搅拌针研究了焊接工艺参数对界面迁移的影响, 发现搅拌头旋转速度增加或焊接速度减小, 返回侧和前进侧界面向上迁移, 焊缝返回侧和前进侧的界面迁移高度随轴肩下压量的增加而增加. Cederqvist L等人^[7]研

究认为, 搭接接头受拉侧界面的垂直迁移量较小时, 接头强度较高; 提高焊接速度、降低旋转速度和缩短搅拌针长度可减小迁移量. 然而目前关于采用右螺纹搅拌针焊接时, 如何控制焊接参数以减小受拉侧界面迁移对接头力学性能的影响很少报道.

文中采用右螺纹圆柱搅拌针, 进行LY12铝合金搅拌摩擦搭接试验, 研究了轴肩下压量对搭接界面迁移的影响.

1 试验方法

试验采用表面带包铝、厚度为3 mm的LY12(CZ)铝合金板进行搅拌摩擦搭接焊试验, 表1为所用LY12铝合金的力学性能. 由于包铝层为纯铝, 耐腐蚀能力与母材有显著不同, 焊接后可通过对试样进行腐蚀, 观察包铝层位置的变化, 分析搭接界面的迁移.

表1 LY12(CZ)铝合金力学性能

Table 1 Mechanical property of LY12(CZ) aluminum

抗拉强度 R_m /MPa	屈服强度 $R_{eL(0.2)}$ /MPa	断后伸长率 δ_{10} (%)
425	227	>12

试验在X53K型立式铣床改装的搅拌摩擦焊机及自制的工装夹具上进行. 搅拌头的轴肩直径为15 mm, 搅拌针为直径5 mm、长度3.3 mm的圆柱型.

收稿日期: 2012-09-05

基金项目: 国家自然科学基金资助项目(50875119); 航空科学基金(20081156009); 江西省自然科学基金(0450090)

焊接过程中,搅拌头向后的倾斜角为 2° ,搅拌头顺时针方向旋转.旋转频率为 750 r/min ,焊接速度 47.5 mm/min ,改变轴肩下压量进行焊接试验.焊后截取焊缝横截面制备金相试样,用keller试剂进行腐蚀,根据焊缝横截面上包铝层的形貌变化,分析搭接界面的迁移.搭接接头的抗剪试验采用如图1所示试样,抗剪强度通过接头断裂载荷与拉断处板材截面积获得.为了分析搭接界面在焊缝厚度方向上的迁移,将4片带包铝层、厚度为 1 mm LY12(CZ)铝合金板水平叠放进行焊接试验,以板材表面的包铝层作为标识材料,观察轴肩下压量对板材厚度方向上焊缝及近缝区金属的流动.

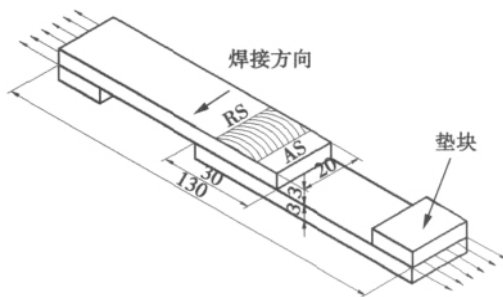


图1 接头拉剪试样(mm)

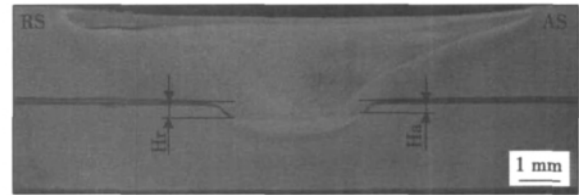
Fig. 1 Tension shear specimen of joint

2 试验结果与分析

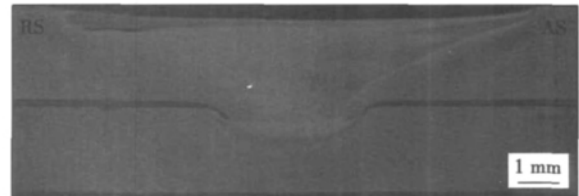
2.1 轴肩下压量对界面迁移的影响

图2为不同轴肩下压量时,焊后接头横截面的宏观形貌.可见,在焊缝中部,原水平连续的搭接界面消失,这是由于搅拌针长度大于板材厚度,且有一定的轴肩下压量,使得搅拌针端部越过搭接界面进入下板,原始界面被搅拌针破碎后在搅拌针后方形形成致密的焊缝;在这个区域的两侧,原始界面朝下板弯曲并伸入到下板形成界面迁移.图2中 H_a 为前进侧(advance side, AS)界面迁移量, H_r 为返回侧(retreating side, RS)界面迁移量.由图2可见,当轴肩下压量大于 0.15 mm 时,如图2a~c所示,焊缝返回侧和前进侧的界面均向下迁移;随轴肩下压量增加,搭接界面向下迁移量增加.当下压量为 0.15 mm 和 0.1 mm 时,宏观上看,焊缝两侧的界面较为平直,没有界面的迁移现象;进一步观察发现,当轴肩下压量为 0.1 mm 时,搅拌针端部靠近前进侧出现了孔洞缺陷.图3为图2e中焊缝两侧界面迁移的放大形貌,可见此时返回侧与焊缝交接处的界面稍向上迁移,前进侧焊缝与搭接界面交接处有明显

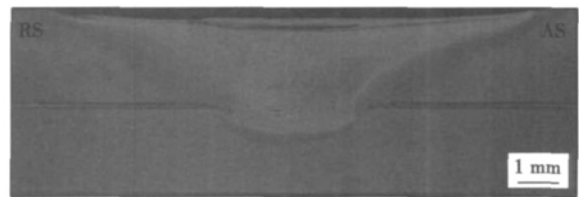
的孔洞.因此,对于文中所用搅拌头,要得到无缺陷的焊缝,轴肩下压量至少应大于 0.1 mm .



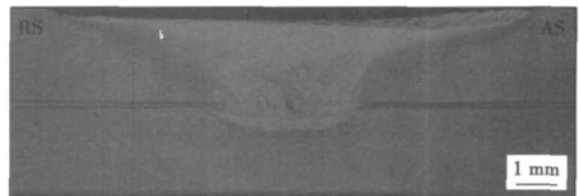
(a) 轴肩下压量 $d=0.3\text{ mm}$



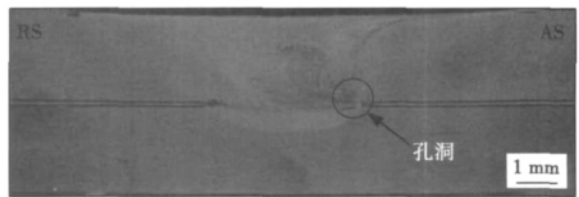
(b) 轴肩下压量 $d=0.25\text{ mm}$



(c) 轴肩下压量 $d=0.2\text{ mm}$



(d) 轴肩下压量 $d=0.15\text{ mm}$



(e) 轴肩下压量 $d=0.1\text{ mm}$

图2 不同轴肩下压量时焊缝的横截面形貌

Fig. 2 Transverse section of weld in various plunge depth of shoulder

2.2 厚度方向不同位置处界面迁移分析

对用厚度为 1 mm 的LY12(CZ)铝合金水平叠加4层的多层板进行搅拌摩擦焊,分析焊缝厚度方向上塑化金属的流动特征.图4为在旋转频率为 750 r/min 、焊接速度为 47.5 mm/min ,不同轴肩下压量时多层板焊缝横截面上标识材料的形貌,其中点划线为焊缝中心位置.由图4可见,焊接过程中,在

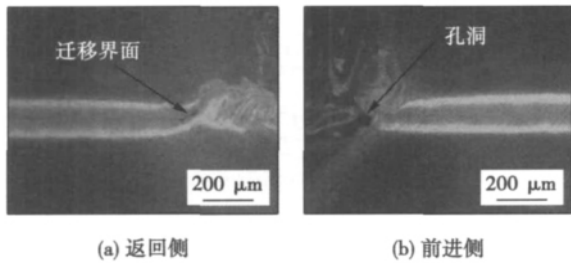


图 3 图 2e 两侧界面迁移的微观形貌

Fig. 3 Micro-morphology of migrated interface at both sides in figure 2e

由上到下的第二、三层界面,搅拌针已将其作用区的界面破碎,原始界面消失并形成焊缝;而焊缝两侧未被破碎的界面发生向下迁移,第二层界面向下迁移较多,第三层界面迁移形貌与图 2a 相似,向下迁移较少。在焊缝上部的第一层界面,返回侧的界面先向下迁移一小段距离后,然后向上迁移,当越过焊缝中心后,几乎呈水平方向迁移到前进侧,焊后界面几乎呈连续、完整形态,仅发生了变形;而前进侧原始界面则在焊核处向下迁移。这表明靠近轴肩的焊缝金属受搅拌头轴肩的旋转作用影响,在搅拌针后方发生返回侧材料向前进侧的迁移;而靠近焊缝前进侧的材料向下迁移。第二层和第三层的界面迁移特征表明,在搅拌针中部,由于搭接界面距离焊缝上表面和搅拌针端部较远,返回侧界面较前进侧有较大的向下迁移;下压量增加时,在同样厚度方向,焊缝两侧界面向下迁移的距离增加;当搭接界面距离搅拌针端部较近时,焊缝两侧界面向下迁移的量较小。

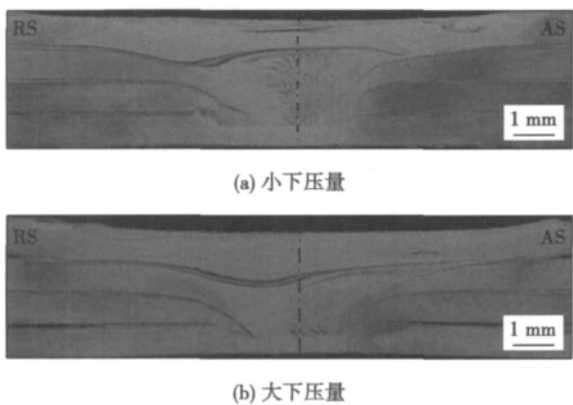


图 4 焊缝横截面上标识材料的形貌

Fig. 4 Appearance of marker in transverse section of weld

搭接焊缝界面迁移反映了搅拌针附近塑性金属的流动状况,这种迁移现象可以用板厚方向上焊缝塑性金属流动的“抽吸-挤压”理论^[8]进行解释。

当搅拌头沿焊接方向运动并以速度 ω 顺时针旋转时,受搅拌针表面螺纹的作用,焊缝塑性金属沿着搅拌针表面上运动,在搅拌针根部聚集并形成塑性金属的挤压区,对周边金属产生挤压效应;同时,由于塑性金属沿搅拌针表面螺纹向上迁移,在搅拌针端部会出现瞬时的低压区或空腔,对周边金属形成抽吸效应。图 5 为搭接界面在这种“抽吸-挤压”作用下迁移的示意图。由图 5 可见,在搅拌针的根部,流出螺纹的塑性金属由于受到轴肩的阻碍,会朝着远离焊缝中心的方向挤压周边金属;受到挤压的塑性金属由于受到离搅拌针较远处温度较低、且未塑化的金属和轴肩的阻碍,只能向下流动,因而在板厚方向上形成了由上向下的迁移,搭接界面在塑性金属这种环形迁移的作用下发生向下迁移。轴肩下压量增加,搅拌头与工件之间的摩擦和顶锻作用增强,使板厚方向上向下迁移的金属量增加。

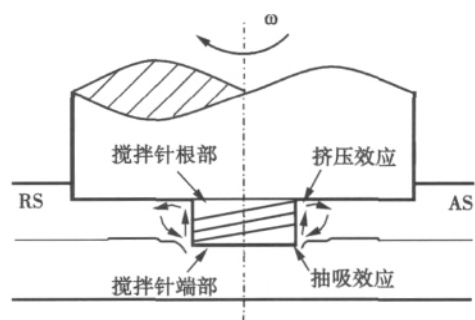


图 5 界面迁移示意图

Fig. 5 Schematic of interface migration

焊缝返回侧和前进侧界面向下迁移的高度不同可能是影响搅拌针两侧塑性金属流动的驱动力不同。图 6 为搅拌针周围塑性区材料流动示意图。焊接时,可将搅拌针的运动分解为沿焊接方向的运动(简称平移)和绕搅拌针中心轴线的旋转运动。图 6a 为搅拌针平移时塑性区材料的流动示意图,其中塑性区域内的箭头表示材料的流动方向。当搅拌针沿焊接方向平移时,搅拌针的前半圆柱面挤压前方的塑性材料使其由两侧(前进侧和返回侧)流向后方,即流动方向为由 I→II 和 IV→III 区。图 6b 为搅拌针旋转运动时塑性区材料的流动示意图,搅拌针顺时针转动时,所有的材料都沿将顺时针方向流动。图 6c 为用运动合成法得到塑性区材料的流动趋势。

上述分析表明,在搅拌针后方塑性区内的金属由两部分金属流组成。在返回侧,这两部分金属流的方向相同;在前进侧,这两部分金属流的方向相反。因此,在焊缝的返回侧可能汇集了比前进侧更

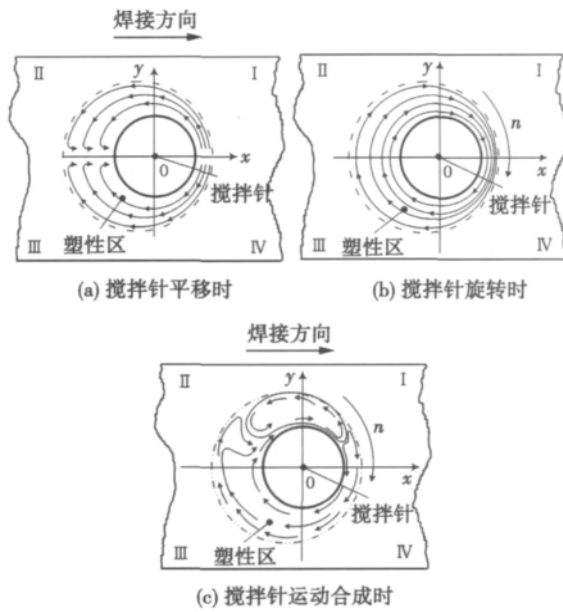


图 6 塑性区材料的流动示意图

Fig. 6 Schematic of material flow trend in plasticized zone

多的塑性金属,使返回侧金属朝下流动更为显著,导致焊接时返回侧搭接界面比前进侧有更大的迁移。

对于搭接焊,搭接界面的迁移形貌还与搅拌针端部离界面的距离有关。当搅拌针端部与界面几乎在同一平面时,搭接界面仅被破碎,焊核两侧的界面没有受到向下的挤压发生向下的迁移;当搅拌针端部深入到搭接界面下方时,搅拌针端部的界面不仅被破碎,而且焊缝两侧的界面会形成较大的向下迁移。如图 4 中第三层界面处,当轴肩下压量较小时,搅拌针端部几乎位于该界面,使该层界面几乎没有向下的迁移;当轴肩下压量增大时,搅拌针端部已到界面下方,使搅拌针端部两侧材料向下流动到搅拌针端部的抽吸区,从而带动界面向下迁移。因此,采用右螺纹搅拌针进行搭接焊时,要减小搭接界面的迁移,需选择合适的搅拌针长度并控制焊接时的轴肩下压量。

2.3 接头力学性能

图 7 8 为不同下压量时搭接接头拉伸断口的横截面形貌,其中白色箭头表示接头的承载方向。从图 7a 可看到,此时焊缝返回侧的界面稍向焊缝中心迁移,而前进侧的界面几乎没有发生迁移。按图 7b 中所示方式加载时,断裂发生在上板的受拉侧(前进侧)。图 7c 是断裂部位的放大图,可见断裂位于焊缝的热力影响区。这是因为下板的受拉侧(返回侧)界面没有明显的向下迁移,外加载荷由无缺口的母材承载,可以承受较大的载荷;而在上板,一方面,较下板受拉边,其承载截面积小;另一方面,此时

承受外加载荷的是焊缝的热影响区,对 LY12(CZ) 铝合金来说,该处材料经焊接加热后,原时效强化的组织会发生软化,其强度低于原始母材^[9],因而断裂发生于上板。因此,对于仅发生微量界面迁移的搭接接头,无论受拉侧是上板前进侧还是返回侧,断裂都发生在上板。

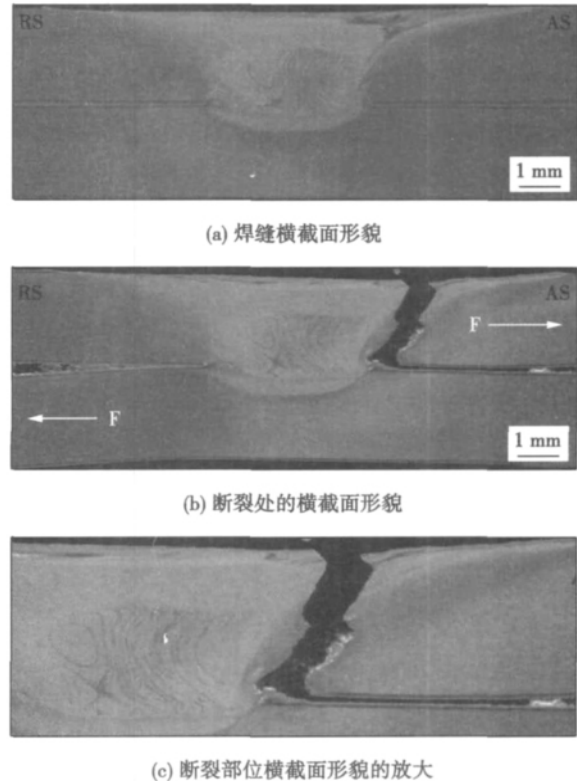


图 7 下压量为 0.11 mm 时的接头断口横截面形貌

Fig. 7 Transverse section of joint's fracture with plunge depth of 0.11 mm

图 8 为轴肩下压量为 0.3 mm 时,搭接接头断口横截面形貌。由图 8 可见,无论受拉侧是上板的前进侧还是返回侧,断裂都发生在下板。这是因为当下压量较大时,焊缝两侧的搭接界面都发生了显著的向下迁移。图 8c 为向下迁移界面的微观形貌。由图 8 可见,伸入到下板的迁移界面并未与母材实现真正的冶金结合,这种未结合的界面使下板的有效承载截面积减小,因而当接头承受载荷时,断裂首先沿迁移界面发生,然后沿垂直载荷的方向形成正断。

图 9 为搭接接头界面迁移高度对接头抗剪强度的影响。可见,下压量较小时,界面向上迁移,迁移量为 0.1 mm,当上板前进侧受拉时,接头的抗剪强度最大(图 7b)。随着界面向下迁移高度的增加,接头抗剪强度下降,并且受拉侧处于下板前进侧时的抗剪强度较受拉侧处于下板返回侧时的抗剪强度高。

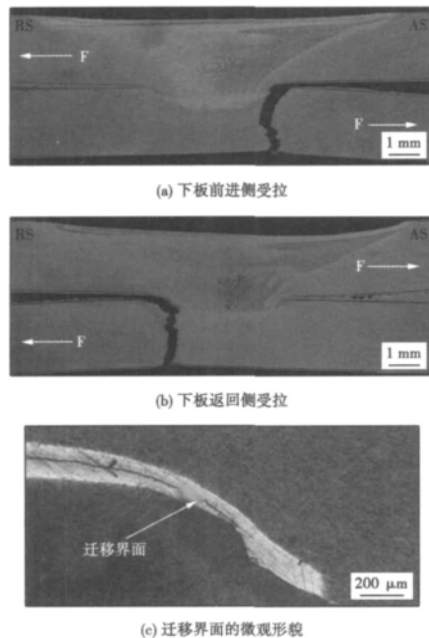


图8 下压量为 0.3 mm 时的接头断口横截面形貌

Fig. 8 Transverse section of joint's fracture with plunge depth of 0.3 mm

(图 8a, b). 这是因为通常返回侧的迁移高度大于前进侧,使得返回侧的有效承载面积减小. 因此,当搅拌针长度不变时,轴肩下压量影响搭接界面的迁移量,以至影响接头的抗剪强度.

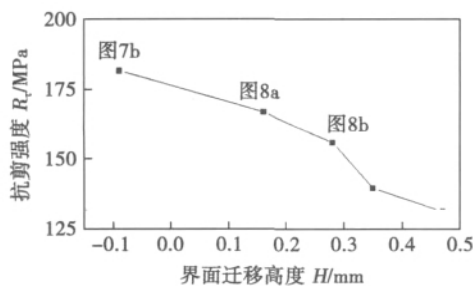


图9 界面迁移高度对接头抗剪强度的影响

Fig. 9 Tension shear strength of joints in different height of interface migration

3 结 论

(1) 采用右螺纹搅拌针焊接,由于沿焊缝厚度方向上的“抽吸-挤压”效应,搭接焊缝两侧产生向下的界面迁移,且焊缝返回侧较前进侧有较大的界面迁移量.

(2) 轴肩下压量较大时,迁移高度随着下压量的增加而增加;当轴肩下压量合适时,焊缝两侧的界面仅发生非常小的向上迁移. 但轴肩下压量太小,

会在焊核两侧产生孔洞缺陷.

(3) 当焊缝两侧界面仅发生较小的向上迁移时,搭接接头有较高的抗剪强度,断裂都发生在上板焊缝的热力影响区,呈正断;焊缝两侧的搭接界面向下迁移时,断裂都发生在下板,接头抗剪强度随界面迁移高度的增加而减小,且受拉侧在下板前进侧时的抗剪强度较受拉侧在下板返回侧时的抗剪强度高.

参考文献:

- [1] Nandan R, Debroy T, Bhadeshia H K D H. Recent advances in friction stir welding process, weldment structure and properties [J]. Progress in Materials Science, 2008, 53(6): 980-1023.
- [2] Buffa G, Campanile G, Fratini L, et al. Friction stir welding of lap joints: Influence of process parameters on the metallurgical and mechanical properties [J]. Materials Science and Engineering A, 2009, 519(1/2): 19-26.
- [3] Xing L, Zou G, Ke L M, et al. Influence of tool pin profile on the interface migration of friction stir lap joints [J]. China Welding, 2011, 20(4): 6-11.
- [4] 柯黎明,魏鹏,邢丽,等. 双道焊对搅拌摩擦焊搭接界面及接头性能的影响 [J]. 焊接学报, 2011, 32(7): 5-8. Ke Liming, Wei Peng, Xing Li, et al. Influence of double passes weld on interface migration and mechanical property of friction stir lap joint [J]. Transactions of the China Welding Institution, 2011, 32(7): 5-8.
- [5] Lee C Y, Lee W B, Kim J W, et al. Lap joint properties of FSWed dissimilar formed 5052 Al and 6061 Al alloys with different thickness [J]. Journal of Materials Science, 2008, 43(9): 3296-3304.
- [6] 魏鹏,邢丽,徐卫平. 轴肩下压量对搅拌摩擦焊搭接焊缝界面迁移的影响 [J]. 材料工程, 2011(6): 43-47. Wei Peng, Xing Li, Xu Weiping. Influence of plunge depth of shoulder on interface migration of friction stir lap welds [J]. Journal of Materials Engineering, 2011(6): 43-47.
- [7] Cederqvist L, Reynolds A P. Factors Affecting the properties of friction stir welded aluminum lap joints [J]. Welding Journal, 2001(80): 281-287.
- [8] 柯黎明,潘际奎,邢丽,等. 搅拌摩擦焊焊缝金属塑性流动的抽吸-挤压理论 [J]. 机械工程学报, 2009, 45(4): 89-94. Ke Liming, Pan Jiluan, Xing Li, et al. Sucking-extruding theory for the material flow in friction stir welds [J]. Journal of Mechanical Engineering, 2009, 45(4): 89-94.
- [9] 刘鹤平,杨成刚,柯黎明. LY12 铝合金搅拌摩擦焊接头组织和性能研究 [J]. 热加工工艺, 2010, 39(15): 139-144. Liu Geping, Yang Chenggang, Ke Liming, et al. Study on microstructure and mechanical properties of friction stir welded joint of LY12 aluminum alloy [J]. Hot Working Technology, 2010, 39(15): 139-144.

作者简介:邢丽,女,1959年出生,教授,硕士研究生导师.主要从事焊接冶金、焊接力学、电弧焊工艺和搅拌摩擦焊技术的教学与科研工作.发表论文50余篇. Email: xingli_59@126.com

MAIN TOPICS ,ABSTRACTS & KEY WORDS

Vacuum high-energy electron beam transient data acquisition and preprocessing SHEN Chunlong^{1,2}, PENG Yong², ZHOU Qi², WANG Kehong² (1. Department Mechanical & Electrical Engineering, Taizhou Teacher College, Taizhou 225300, China; 2 School of Materials Science & Engineering, Nanjing University Science & Technology, Nanjing 210094, China). pp 1-4

Abstract: High-energy electron beam power density distribution and its spatial pattern are important factors for the quality of electron beam. On the basis of analyzing the characteristics of high-energy electron beam, a novel electron beam testing method and testing device were proposed. Based on characteristics and the relationship between electron beam deflection signal and scanning signal, a signal acquisition structure was developed. High-frequency, high-speed data transfer, sharing of external clock source and acquisition trigger mode were dealt with a PCI-1714 card. Serial communication, data collection process and segmentation preprocess method were described in detail. The results show that the developed system could effectively capture the original high-energy transient signal of electron beam, which provided a method for analysis and processing of electron beam spatial data.

Key words: vacuum; electron beam; power density distribution; data acquisition

Numerical simulation of transient keyhole instability and weld pool behaviors in parallel dual-beam laser welding Part I. Model development and transient keyhole behaviors

CHEN Weidong, PANG Shengyong, LIAO Dunming, ZHOU Jianxin (State Key Laboratory of Materials Processing and Die & Mould Technology, Huazhong University of Science and Technology, Wuhan 430074, China). pp 5-9

Abstract: A three-dimensional mathematical model is proposed to simulate the transient keyhole instability and weld pool behaviors in parallel dual-beam laser welding. It is shown that one or two keyholes might be created and the evolution of keyholes is complicated during parallel dual-beam welding. The development of keyhole depth could be characterized as three phases and periodic. The frequency of keyhole depth oscillation in parallel dual-beam welding is several kHz, which is in the same order of magnitude in single laser welding. It is also found that the amplitude of keyhole depth oscillation decreases as the welding speed increases, and the keyhole could even be stable if the welding speed is large enough. Moreover, it is shown that the amplitude of keyhole depth oscillation increases if the interbeam distance is too large or too small, and penetration fluctuation is found when the interbeam distance is too large.

Key words: parallel dual beam laser welding; transient keyhole instability; weld pool behaviors; mathematical model

Process parameters optimization of nanostructured ZrO₂-7%Y₂O₃ coating deposited by plasma spraying based on genetic algorithms and neural networks WANG Dongsheng^{1,2}, YANG Bin², TIAN Zongjun¹, SHEN Lida¹, HUANG Yinhui¹ (1. College of Mechanical and Electrical Engineering, Nanjing University of Aeronautics and Astronautics, Nanjing 210016, China; 2. Department of Mechanical Engineering, Tongling University, Tongling 244000, China). pp 10-14

Abstract: BP neural networks and genetic algorithms were combined to optimize process parameters of the nanostructured ZrO₂-7%Y₂O₃ coating prepared by plasma spraying technique. The neural networks were trained based on the experimental results of orthogonal tests, and the BP neural networks model was developed to describe the relationship between coating properties (bonding strength and microhardness) and four main process parameters, including spraying distance, spraying electric current, primary gas pressure and secondary gas pressure. Meanwhile, the bonding strength and microhardness of the nanostructured coating were optimized with single-objective and multi-objective optimization methods based on the genetic algorithms. The results show that the prediction data agrees well with the experimental values, which indicates that the proposed model is correct and reliable. The maximum bonding strength and microhardness of the coating are 44 MPa and 1 266 HV, respectively. The overall performance of the coating is best when the spraying distance is 90.66 mm, spraying electric current 934.63 A, primary gas pressure 0.302 MPa and secondary gas pressure 0.892 MPa while keeping the weight of bonding strength and microhardness constant.

Key words: plasma spraying; nanostructured coating; neural networks; genetic algorithms; process parameters optimization

Influence of plunge depth of shoulder on mechanical properties of friction stir lap joints XING Li, WEI Peng, SONG Xiao, KE Liming (National Defense Key Disciplines Laboratory of Light Alloy Processing Science and Technology, Nanchang Hangkong University, Nanchang 330063, China). pp 15-19

Abstract: Friction stir welding (FSW) lap joints of 3 mm-thick LY12 aluminum alloy sheets were made using a cylindrical tool with right-hand threaded pin, and the effects of plunge depth of shoulder on the interface migration and mechanical properties of resultant joints were investigated. The results show that the lap interfaces on both sides of weld nugget moved downward, and the height of interface migration rose with increase of plunge depth of shoulder. The height of interface migration was greater on the retreating side than on the advancing side. The interfaces on both sides of weld moved slightly when using an appropriate plunge depth of shoulder. The shear strength of lap

joint was excellent due to the slight interface migration , and fracture occurred in the top sheet. However , when the interfaces at both sides of weld moved downward , fracture occurred in the bottom sheet. The shear strength decreased with increase of the height of interface migration. The shear strength was higher when the load was exerted on the advancing side than on the retreating side.

Key words: friction stir welding; lap joint; plunge depth of shoulder; interface migration; mechanical properties

Effects of welding parameters on temperature field in GTAW ZHAO Ming , DU Dandan , LUO Detong (College of Mechanical and Electronic Engineering , China University of Petroleum , Qingdao 266580 , China) . pp 20 – 24

Abstract: Numerical analysis of heat transfer in gas tungsten arc welding (GTAW) process was conducted with ANSYS software. The calculated results of transient evolution of isotherms during continuous welding for 20 s and cooling for 20 s show that the workpiece was completely penetrated at 5 s after the arc was struck , however , the molten pool totally disappeared within 1 s after the arc moved away. During the welding process , the high-temperature region moved simultaneously with the arc. When the arc moved away , the cooling stage began , the zone with high temperature gradually moved backward (relative to the welding direction) and cooled to ambient temperature. The predicted thermal cycles at different points with the same intervals on top surface along the welding direction displayed that the temperature rising curves have the same trend in quasi-steady state , while clear differences existed between the temperature decreasing curves because the latent heat was released when the molten metal solidified. The temperature decreased faster at points closer to the weld crater. The influences of welding current , welding speed and concentration parameter on the heat transfer were analyzed , and then these parameters were optimized.

Key words: Gaussian heat source; distribution parameter of heat flux; gas tungsten arc welding; numerical analysis

Microstructure and mechanical properties in heat-affected zone of large-thickness steel ingot cut with oxygen-propane flame HAN Yongkui¹ , WANG Zhixin¹ , YAN Jiashu¹ , LIN Yaowu² , ZHAO Xianhong² , MEI Longtian² (1. Harbin Welding Institute , China Academy of Machinery Science and Technology , Harbin 150080 , China; 2. HengDing Shipbuilding Heavy Industry Co. , Ltd. , Suzhou 215513 , China) . pp 25 – 28 , 32

Abstract: The machining allowance of precision metal cutting machine tools depends on the microstructure evolution in heat-affected zone during flame cutting. In this paper , 900 mm thick 34CrNiMo6 steel and 450 mm thick 45 carbon steel ingots were cut using an oxygen-propane flame. Then , the macroscopic morphology and microstructure in the heat-affected zone were examined to analyze the influence of microstructure evolution on the performance of workpieces. The range of heat-affected zone and machining allowance were determined to optimize the parameters during cutting and after cutting process.

Key words: flame cutting; large cross-section; steel; microstructure; heat-affected zone

Fatigue crack propagation of aluminum alloy based on acoustic emission monitoring ZHU Ronghua , GANG Tie (State Key Laboratory of Advanced Welding and Joining , Harbin Institute of Technology , Harbin 150001 , China) . pp 29 – 32

Abstract: The acoustic emission technique was used to monitor the fatigue crack propagation of 7N01 aluminum alloy single-edge notched three-point bend specimens under different stress ratio and peak load. The relationship between the crack growth rate , acoustic emission count rate and stress intensity factor range was established. The results show that most of the acoustic emission signals were produced in the low stress cyclic loading stage because the acoustic emission activity in low-stress phase was mainly related to the plastic deformation and crack closure in crack tip , and the acoustic emission count exponentially grew with the stress intensity factor. Based on the relationship between the acoustic emission count rate and crack growth rate , the remaining life of fatigue-damaged structures could be predicted.

Key words: aluminum alloy; acoustic emission; fatigue; counts

Arc pressure measurement and analysis of coupling arc AA-TIG HUANG Yong^{1,2} , QU Huaiyu¹ , FAN Ding^{1,2} , LIU Ruilin¹ , KANG Zaixiang¹ , WANG Xinxin¹ (1. State Key Laboratory of Gansu Advanced Non-ferrous Metal Materials , Lanzhou University of Technology , Lanzhou 730050 , China; 2. Key Laboratory of Non-ferrous Metal Alloys , The Ministry of Education , Lanzhou University of Technology , Lanzhou 730050 , China) . pp 33 – 36

Abstract: In order to study the coupling arc AA-TIG (arc assisted activating tungsten inert gas) welding , a static keyhole method was used to measure the arc pressure with stainless steel as the anode. The influence of main process parameters on the distribution of arc pressure was analyzed. Compared to the conventional TIG welding process under the same conditions , the peak value of arc pressure during the coupling arc AA-TIG welding was significantly reduced. With the welding current decreasing , the electrode distance increasing , the arc length increasing and the oxygen content of the assisted arc decreasing , the peak value of arc pressure in coupling AA-TIG welding decreased. The distribution of arc pressure was in concordance with Gaussian distribution at 2 mm electrode distance. With the electrode distance increasing , the distribution gradually turned into bimodal distribution.

Key words: AA-TIG; coupling arc; oxygen element; arc pressure; high-speed welding

Influence of weld shaping with trailing impact rolling on hardness and residual stress of under-matched equal load-carrying joint YANG Jianguo¹ , WANG Jiajie² , DONG Zhibo² , FANG Hong yuan² , ZHOU Lipeng³ (1. Institute of Process Equipment and Control Engineering , Zhejiang University of Technology , Hangzhou 310014 , China; 2. State Key Laboratory of Advanced Welding and Joining , Harbin Institute of Technology , Harbin 150001 , China; 3. CGNPC Inspection Technology Co. Ltd , Suzhou 215004 , China) . pp 37 – 40